Published in the proceedings of the European Conference of Computer Vision (ECCV'96), April 14-18, 1996, Cambridge, England

Tracking medical 3D data with a deformable parametric model

Eric Bardinet[1], Laurent Cohen[2] and Nicholas Ayache[1]

[1] Epidaure project, INRIA
2004 Route des Lucioles, B.P. 93 06902 Sophia Antipolis CEDEX, France.
[2] Ceremade, Université Paris IX - Dauphine
Place du Marechal de Lattre de Tassigny 75775 Paris CEDEX 16, France

Abstract. We present a new approach to surface tracking applied to 3D medical data with a deformable model. It is based on a parametric model composed of a superquadric fit followed by a Free-Form Deformation (FFD), that gives a compact representation of a set of points in a 3D image. We present three different approaches to track surfaces in a sequence of 3D cardiac images. From the tracking, we infer quantitative parameters which are useful for the physician, like the ejection fraction, the variation of the heart wall thickness and of the volume during a cardiac cycle or the torsion component in the deformation of the ventricle. Experimental results are shown for automatic shape tracking and motion analysis of a time sequence of Nuclear Medicine images.

1 Introduction

The analysis of cardiac deformations has given rise to a large amount of research in medical image understanding. Indeed, cardiovascular diseases are the first cause of mortality in developed countries. Various imaging techniques make it possible to get dynamic sequences of 3D images (**3**D+T). The temporal resolution of these techniques is good enough to obtain a sufficient number of images during a complete cardiac cycle (contraction and dilation). These images are perfectly adapted to study the behavior of the cardiac system since they visualize how the heart walls deform. Processing these images opens numerous fields of applications, like the detection and analysis of pathologies.

The recent techniques of imagery, like Nuclear medicine data and Scanner, provide more and more precise resolution in space as well as in time. This means that the data available to the radiologist are larger and larger. To establish a reliable and fast diagnosis, the physician needs models that are defined by a small number of characteristic quantities.

Since it is characteristic of the good health of the heart, the left ventricle motion and deformation has been extensively studied by medical image processing groups as well as hospitals. Since its creation in 1989, our group has pioneered work in the use of deformable models to extract the left ventricle [2, 6, 5]. Other groups as well have also given various contributions to the understanding of the complex deformation of the ventricle [1, 9, 10, 11].

A parametric model is weel-suited when dealing with a huge amount of data like for object tracking in a sequence of 3D images. In a previous paper [3], we introduced a parametric deformable model based on a superquadric fit followed by a Free-Form Deformation (FFD). We show in this paper how we use this parametric model to make an efficient tracking of the LV wall in a sequence of 3D images. The reconstruction and representation of a time sequence of surfaces by a sequence of parametric models will then allow to infer some characteristic parameters which are useful for the physician, like the ejection fraction, the variation of the heart wall thickness and of the volume during a cardiac cycle or the torsion component in the deformation of the ventricle.

2 A parametric model to fit 3D points

In this section, we sketch the deformable model that we use for efficient tracking of the cardiac left ventricle. For more details and references on the complete algorithm, see [3]. In brief, we first fit 3D data with a superellipsoid, and then refine this crude approximation using Free Form Deformations (FFDs).

2.1 Fitting 3D data with superquadrics

The goal of the algorithm is to find a set of parameters such that the superellipsoid best fits the set of data points. Superquadrics form a family of implicit surfaces obtained by extension of conventional quadrics. Superellipsoids are defined by the implicit equation:

$$\left(\left(\left(\frac{x}{a_1}\right)^{\frac{2}{\epsilon_2}} + \left(\frac{y}{a_2}\right)^{\frac{2}{\epsilon_2}}\right)^{\frac{\epsilon_2}{\epsilon_1}} + \left(\frac{z}{a_3}\right)^{\frac{2}{\epsilon_1}}\right)^{\frac{\epsilon_1}{2}} = 1. \tag{1}$$

Suppose that the data we want to fit with the superellipsoid are a set of 3D points $(x_d, y_d, z_d), i = 1, \cdots, N$. Since a point on the surface of the superellipsoid satisfies $F = 1$, where F is the function defined by equation (1), we seek for the minimum of the following energy (see [3] for a geometric interpretation):

$$E(A) = \sum_{i=1}^{N} \left[1 - F(x_d, y_d, z_d, a_1, a_2, a_3, \epsilon_1, \epsilon_2)\right]^2 . \tag{2}$$

2.2 Refinement of the fit with Free Form Deformations (FFDs)

To refine the previous parametric representation, we use a global volumetric deformation called FFD. The main interest of FFDs is that the resulting deformation of the object is just defined by a small number of points. This typical feature allows us to represent voluminous 3D data by models defined by a small number of parameters.

Definition of FFDs FFDs are an application from $\mathbb{R}^3$ to $\mathbb{R}^3$, defined by the tensor product of trivariate Bernstein polynomials. This can be written in a matrix form: $\boldsymbol{X} = \boldsymbol{BP}$, where $\boldsymbol{B}$ is the deformation matrix $ND \times NP$ (ND: number of points on the superellipsoid, NP: number of control points), $\boldsymbol{P}$ is a matrix $NP \times 3$ which contains coordinates of the control points and $\boldsymbol{X}$ is a matrix $ND \times 3$ with coordinates of the model points (see [3] for details).

The inverse problem The superellipsoid fit provides a first parametric approximation of the set of 3D data, which is often a crude one. We use FFDs to refine this approximation. Therefore we need to solve the inverse problem: first compute a displacement field $\delta \boldsymbol{X}$ between the superellipsoid and the data, and then, after having put the superellipsoid in a 3D box, search the deformation $\delta \boldsymbol{P}$ of this box which will best minimize the displacement field $\delta \boldsymbol{X}$:

$$\min_{\delta \boldsymbol{P}} \|\boldsymbol{B}\delta\boldsymbol{P} - \delta\boldsymbol{X}\|^2 \tag{3}$$

Simultaneous deformation of two surfaces An essential feature of this algorithm is that FFD is a volumetric deformation. This means that several objects can be deformed simultaneously with only one FFD. Using only one model means that the two surfaces are put in a same control point box, and the minimization of equation (3) is done simultaneously on the union of both displacement fields. Moreover, our model gives an interpolation of the 3D deformation everywhere in the volume between the two surfaces. Figure 4 shows the result of the algorithm

	Separate computation	Simultaneous computation
Epicardium	0.007448	0.008236
Endocardium	0.012838	0.014376

Table 1. Least-square errors $\|\boldsymbol{BP} - \boldsymbol{X}\|$ between original data and parametric models. Left column: each model is computed independently. Right column: the two models are computed with one FFD.

for the reconstruction of the epicardium and the endocardium, simultaneously computed with only one FFD. The approximation errors, corresponding to the computation using two FFDs or only one FFD, are presented table 1. One can see that using two FFDs for the two surfaces leads to a better quality of approximation. On the other hand, using only one FFD allows to reduce the number of parameters by half, yielding to a larger compression of the information needed for the description of the parametric model. It also permits to infer from this single FFD, a deformation field over the entire space, due to the volumetric formulation of FFDs. In the particular case of cardiac deformations, it allows to estimate the deformation of any point included in the volume between the epicardium and the endocardium, namely the myocardium.

We show in Figure 1 the effect of the Free Form Deformation applied on the volume between the two superellipsoids. To visualize this volume information, we show the image of segments linking these two surfaces. The FFD being computed to obtain simultaneously the epicardium and the endocardium surfaces deforms also the segments that link the surfaces.

3 Dynamic tracking of the left ventricle

In this section, we apply this model to the tracking of the left ventricle in SPECT cardiac images.

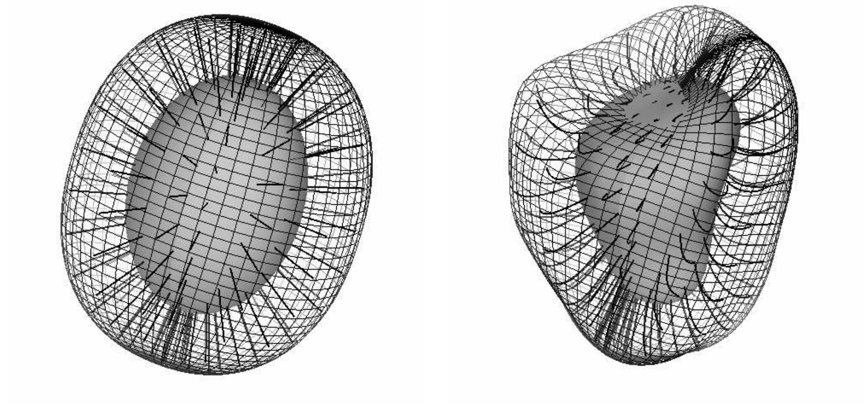

Fig. 1. Volumetric deformation. FFD previously computed simultaneously from the two isosurfaces is applied to rigid links between the superellipsoid models and provides an elastic volumetric deformation of the myocardium.

3.1 Dealing with a time sequence

General deformable models usually need an initialization that is close enough to the solution. This is well suited for tracking in medical images since the deformation between two images is small and the model can start with the solution in the previous image as initialization for the current one.

With our parametric deformable model, the initialization is made automatically through the superquadric fit (see section 2.1), and then refined by the FFD. It is thus possible to make the reconstruction of each data set independently. However, having a previous refined model permits us to get an increasing precision in the reconstruction. This leads to three possible approaches for tracking that are presented in figure 2.

Independent representation This first approach consists of applying to each 3D image the complete model. The advantage is that to define the model at time n, we do not need any previous model information but only the superellipsoid and the control point box for this data.

This approach does not make use of the fact that the results at time n is close to the already computed one at time $n-1$. This means that there is not a temporal processing but a successive computation of static frames.

Recursive representation This method is a real temporal tracking. The complete model is applied only to the data of the first image, and then for time n, the model is obtained from the one at time $n-1$. This means that the shape obtained at time $n-1$ is itself put into a control point box instead of a superellipsoid in section 2.2. It results that the surface at time n is obtained from the

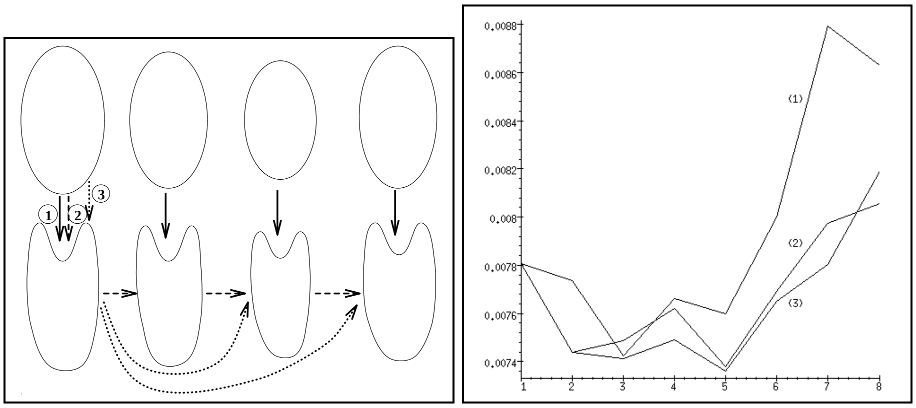

Fig. 2. Left: three different approaches to deal with a temporal sequence. 1 : Data reconstruction at each time step using the superquadric and FFD fit. 2 : Data reconstruction at time step n using the FFD from the model found at time $n-1$. 3 : Data reconstruction at time step n using only the FFD from the model found at time 1. Right: time evolution of the least square error between the data and model for the 8 frames. The three curves correspond to the three approaches. The larger error is obtained with approach 1.

superellipsoid at time 1 iteratively deformed by the sequence of the n first control point boxes. This has the advantage of being more and more precise when time increases since an accumulation of boxes allows the reconstruction of more complex shapes. However, since all previous boxes are needed to reconstruct the data at time n, this may be a difficulty when dealing with a long sequence of images.

Independent representation with a reference deformation The third approach is a trade-off between the two previous ones. The complete model is applied only to the data of the first image, and then for time n, the model is obtained from the one at time 1. This means that the first reconstruction at time 1 is considered as a reference deformation of the superellipsoid. At time n, this reference shape is put into a control point box like in section 2.2. It results that the surface at time n is obtained from the superellipsoid at time 1, followed by two deformations defined by the reference control point box and the current box. This has the advantage of both previous approaches. The approximation is more precise, being the iteration of two boxes and each data set can be retrieved from only one box and the first box and superellipsoid parameters. This is thus independent of the length of the time sequence.

Since in practical applications, this method is as precise as the second one, as shown in figure 2, this is the one we have chosen for the result presented in the next section.

3.2 Application to the left ventricle tracking in spatio-temporal data (3D+T)

We present in this section applications of the tracking algorithm on 3D+T cardiac images.

The models were computed on the following time sequence: Nuclear medicine data (SPECT sequence), with 8 successive time frames during one cardiac cycle. Each image is a volume of $64 \times 64 \times 64$ voxels. The original 3D images are visualized as a series of 2D cross-sections (according to the Z axis) in figure 3.

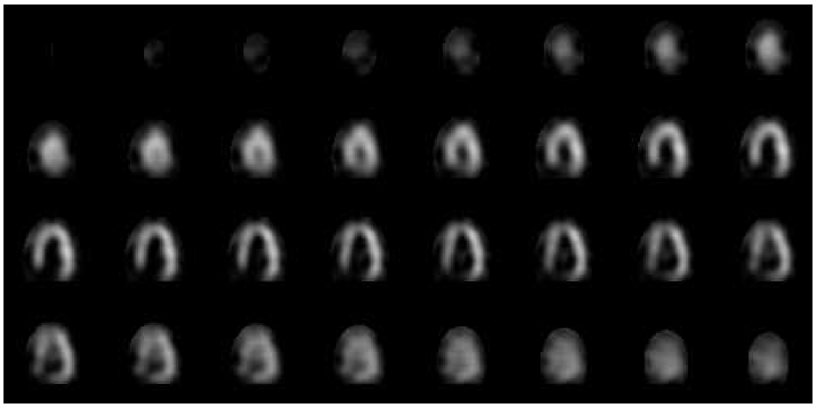

Fig. 3. 3D image of the left ventricle (SPECT data). Order of sections: from left to right and from top to bottom.

Morphological segmentation and representation of the data In order to get time sequences of 3D points which correspond to the anatomical structure that we want to track (epicardium and endocardium of the cardiac left ventricle), and therefore fit our model on these sets of points, we have to segment the original data. As one can visually remark on Figures 3, this is not an easy task because the SPECT images are quite noisy.

To obtain an accurate and robust segmentation, we must combine thresholding with mathematical morphology and connected components analysis (as in Hoehne [8]). We first choose a threshold which grossly separates the ventricle (high values) from the rest of the image. The same value is chosen for the whole sequence of images. Then we extract the largest connected component for each of the resulting 3D binary images, and perform a equal number of erosions and dilations (morphological closings). This last operation is necessary to bridge little gaps and smooth the overall segmentation. Finally, the extraction of the sequence of isosurfaces from that last sequence of images provides the sequence of sets of 3D points that we need as input for the complete reconstruction and tracking algorithm.

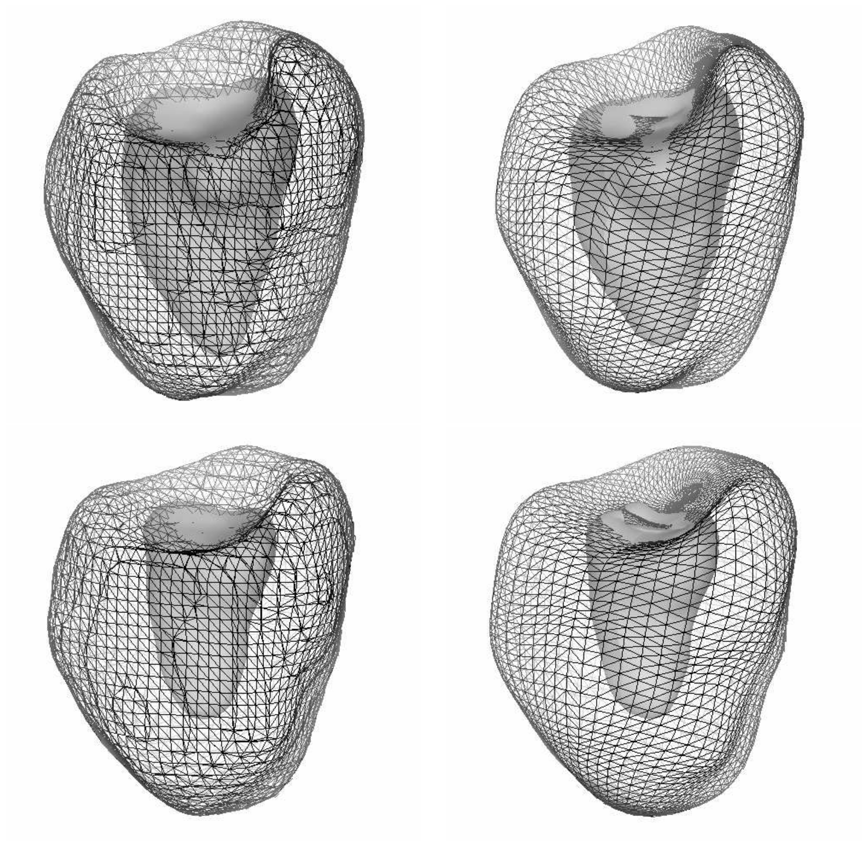

Fig. 4. Time sequence of the epicardium and the endocardium. Left: isosurfaces obtained by data segmentation (4500 + 1500 points). Right: representation by two parametric models (2×130 parameters).

To understand the complex behavior of the cardiac muscle, we have to recover the deformations of both the internal and external walls of the myocardium, namely the endocardium and the epicardium. It is possible to represent the complete myocardium by only one deformable superellipsoid-based model (as in Figure 2). However, by recovering the large concavity which corresponds to the ventricular cavity, which means a strong displacement constraint, it follows that all the other constraints are negliged, thus involving a smoothing effect on the surface model. On the other hand, the shape of the myocardium looks very much like two deformed concentric ellipsoids, and it is thus natural to use two models to recover the two cardiac walls.

Figure 4 represents the dynamic sequence of the segmented and reconstructed surfaces, using one model as explained in Section 2.2.

3.3 Quantitative analysis

The reconstruction and representation of a time sequence of surfaces by a sequence of parametric models permits to extract some characteristic parameters and give interpretation or diagnosis on the patient. In the major domain of cardio-vascular diseases, and especially to study the cardiac muscle, the useful parameters for diagnosis are mainly the ejection fraction, the variation of the heart wall thickness and of the volume during a cardiac cycle or the torsion component in the deformation of the ventricle. Similar parameters are also obtained in the work of [10] to quantify the left ventricle deformation.

With this goal in mind, we use our sequence of models to compute the volume of the ventricular cavity, and also to extract the time trajectory of each point of the surface during a cardiac cycle. The assumption made is that the deformation of a point in the parameterization of the surface corresponds to the deformation of the material point of the tissue. Of course, some other constraints could be added to get a better correspondance between the two physical surfaces. In [2, 5], local geometrical properties based on curvature are used to improve the matching between two curves, surfaces or images in a context of registration. However since the deformation is nonrigid, the differential constraints are not always very significant.

Volume evolution To evaluate the ejection fraction, we need a way to compute the evolution in the time sequence of the ventricle cavity volume. We use the discrete form of the Gauss integral theorem to calculate the volume of a region bounded by a grid of points. More details on this formula can be found in [4]. We applied this calculation of endocardium volumes to the sequences of both data points and parametric models obtained in the previous sections. Once we have the values of the volume along a cardiac cycle, we can easily obtain the ejection fraction (calculated precisely as : $\frac{Vd - Vc}{Vd}$, with Vd volume at dilation (end diastole), Vc volume at contraction (end systole), see for example [7]. The results presented in figure 5 show that:

- The evolution of the volume has the expected typical shape found in medical litterature [7]. Moreover, estimation of the ejection fraction on our example gives a value of 68%, that is in the range of expected values from medical knowledge [7].
- The volumes found for data and models are almost identical as seen from the error curve. The relative average error along the cycle is 0.42%. This proves that our model is robust with respect to the volume estimation. Of course, the ejection fraction is also obtained with a very small relative error (0.19%).
- The volume evolution found for initial superellipsoid models before FFD, have also a very similar shape. However, there is a size ratio due to the overestimation of the volume before the FFD. This ratio is almost constant in time, which makes possible to get a good estimate of the ejection fraction directly from the initial model. This proves that the superellipsoid model

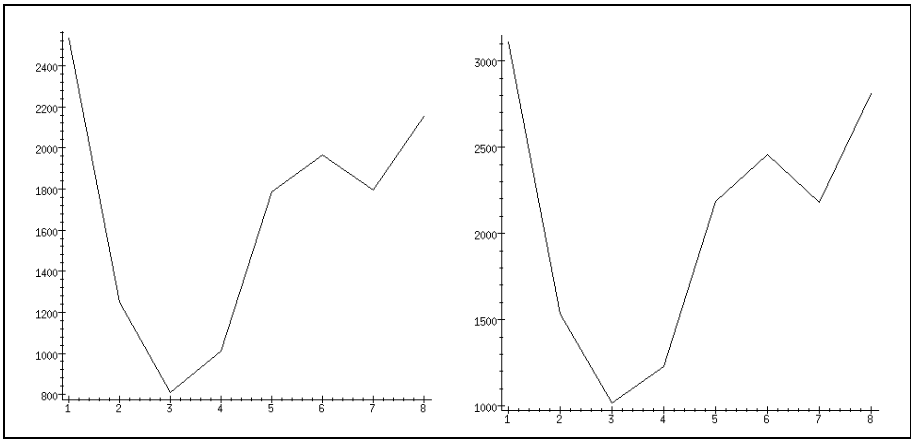

Fig. 5. Endocardium volume during the cardiac cycle. Left: volume of the data. Right: volume of the superellipsoid model.

provides a good global estimate of the shape. Also, the volume of the superellipsoid can be obtained analytically from its set of parameters without the previous discrete approximation (for details, see [4]).

Trajectories Listing the successive positions of a parametric point of the deformed surface model along the time sequence, we obtain the trajectory followed by this point. Figure 6 shows the trajectories of the node points between the end diastole and the end systole. One can see that the model catches the characteristic twist component of the motion. This torsion has been quantified by the decomposition of the displacement vectors in cylindrical coordinates:

$$\begin{pmatrix} x \\ y \\ z \end{pmatrix} \rightarrow \begin{pmatrix} \rho = \sqrt{x^2+y^2} \\ \theta = Arcos(\frac{x}{\sqrt{x^2+y^2}}) \\ z = z \end{pmatrix} \tag{4}$$

The z-axis for the cylindrical representation correspond to the z-axis of inertia of the superellipsoid model. To measure the torsion, we compute the difference of the θ parameters for the two points that represent the same parametric point during the contraction, Figure 7 represents the mean values of $\theta' - \theta$ (in radians) along the different latitudes. One can see that the torsion is in the range 10 - 12 degrees which is the expected range.

The pointwise tracking of the deformation permits to give an evaluation of the velocity field during the sequence. The visualization of these displacements by different colors, according to their range, on the surface shows up clearly areas on the ventricle where the deformation is weak (see Figure 6). This visualization could be used by the physician to help localize pathologies like infarcted regions.

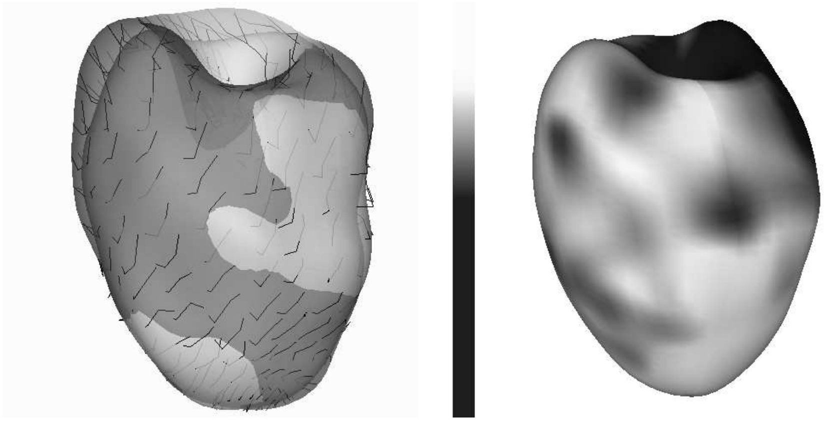

Fig. 6. Left: trajectories of the model's points during a cardiac cycle. The two surfaces represent the the models at end of diastole (dilation) and systole (contraction). Right: range of the displacements of the model's points during a cardiac cycle.

Wall thickness Another important feature that is useful for the diagnosis is the evolution of the wall thickness during the cardiac contraction. Computing only one model to recover the deformation of both the epicardium and the endocardium permits to calculate easily this parameter. Figure 7 shows the evolution of the wall thickness over time for a given point. This thickness has been computed as the difference of the ρ parameters for two parametric points on the epicardium and the endocardium. Figure 8 represents the volumetric deformation of a volume element inside the myocardium muscle. This element is defined by two corresponding rectangle elements on each of the two parameterized surfaces (epicardium and endocardium). The nodes of these rectangles are linked by curvilinear segments that show the volumetric effect of the FFD (see Section 2.2).

4 Conclusion

We presented a new approach to surface tracking applied to 3-D medical data with a deformable model. It is based on a parametric model that gives a compact representation of a set of points in a 3-D image. Three approaches were presented to use this model in order to track efficiently the left ventricle walls in a sequence of 3D images during a cardiac cycle. The model is able to track simultaneously the endocardium and the epicardium. Experimental results have been shown for automatic shape tracking in time sequences.

The reconstruction and representation of a time sequence of surfaces by a sequence of parametric models has then permitted to infer some characteristic parameters which are useful for the physician.

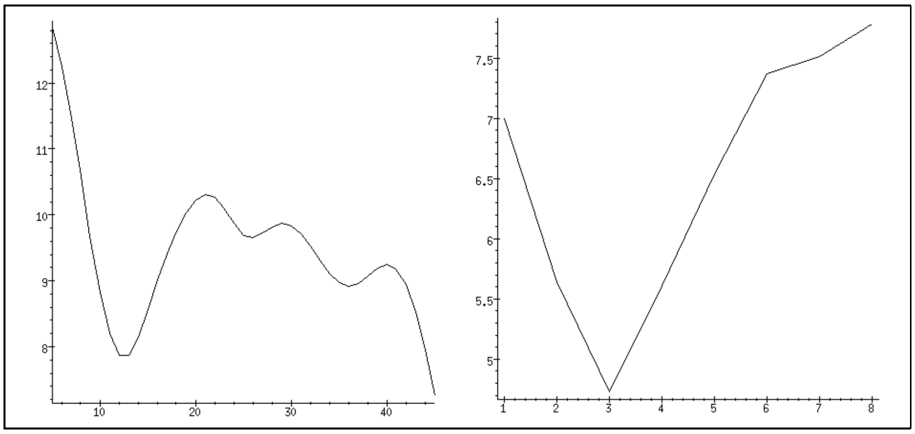

Fig. 7. Left: mean torsion during the cardiac cycle along the z-axis (0 and 50 represent the two poles of the parameterization). Right: evolution of the wall thickness during the cardiac cycle for one point of the volumetric model.

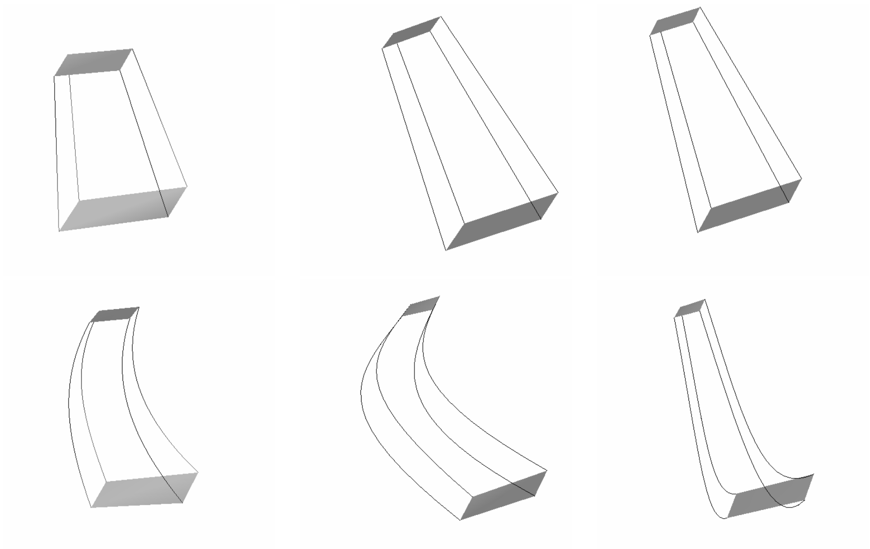

Fig. 8. Volumetric deformation of a volume element inside the myocardium during the cardiac cycle (3 time steps). Top: volume element between the superellipsoid models. Bottom: volume element between the final models, after the volumetric deformation.

We currently consider adding to our work hard displacement constraints like the ones available from the recent imaging technique denoted tagged MRI.

References

1. A. Amini, R. Owen, P. Anandan, and J. Duncan. Non-rigid motion models for tracking the left ventricular wall. In *Information processing in medical images*, Lecture notes in computer science, pages 343–357, 1991. Springer-Verlag.
2. N. Ayache, I. Cohen, and I. Herlin. *Medical Image Tracking*, chapter 20. MIT Press, 1992.
3. E. Bardinet, L. Cohen, and N. Ayache. Fitting of iso-surfaces using superquadrics and free-form deformations. In *Proceedings IEEE Workshop on Biomedical Image Analysis (WBIA)*, Seattle, Washington, June 1994.
4. E. Bardinet, L.D. Cohen, and N. Ayache. Analyzing the deformation of the left ventricle of the heart with a parametric deformable model. Research report, INRIA, Sophia-Antipolis, February 1996. (to appear).
5. S. Benayoun, C. Nastar, and N. Ayache. Dense non-rigid motion estimation in sequences of 3D images using differential constraints. In *Proceedings Conference on Computer Vision, Virtual Reality and Robotics in Medecine (CVRMed)*, pages 309–318, Nice, France, April 1995.
6. L.D. Cohen and I. Cohen. Finite element methods for active contour models and balloons for 2-D and 3-D images. *IEEE Transactions on Pattern Analysis and Machine Intelligence*, 15(11), November 1993.
7. M. Davis, B. Rezaie, and F. Weiland. Assessment of left ventricular ejection fraction from technetium-99m-methoxy isobutyl isonitrile multiple-gated radionuclide angiocardoigraphy. *IEEE Transactions on Medical Imaging*, 12(2):189–199, June 1993.
8. K. Höhne and W. Hanson. Interactive 3D segmentation of MRI and CT volumes using morphological operations. *Journal of Computer Assisted Tomography*, 16(2):285–294, March 1992.
9. D. Metaxas and D. Terzopoulos. Shape and nonrigid motion estimation through physics-based synthesis. *IEEE Transactions on Pattern Analysis and Machine Intelligence*, pages 580–591, June 1993.
10. J. Park, D. Metaxas, and A. Young. Deformable models with parameter functions : application to heart-wall modeling. In *Proceedings IEEE Computer Society Computer Vision and Pattern Recognition (CVPR)*, pages 437–442, June 1994.
11. P. Shi, A. Amini, G. Robinson, A. Sinusas, C. Constable, and J. Duncan. Shape-based 4D left ventricular myocardial function analysis. In *Proceedings IEEE Workshop on Biomedical Image Analysis (WBIA)*, pages 88–97, Seattle, June 1994.

This article was processed using the LaTeX macro package with ECCV'96 style